Chin. Geogra. Sci. 2022 Vol. 32 No. 5 pp. 792−807
https://doi.org/10.1007/s11769-022-1301-5

Springer Science Press
www.springerlink.com/content/1002-0063

Differentiation of Algal Blooms and Aquatic Vegetation in Chinese Lakes Using Modified Vegetation Presence Frequency Index Method

PU Jing[1], SONG Kaishan[2], LIU Ge[2], WEN Zhidan[2], FANG Chong[2], HOU Junbing[2], LV Yunfeng[1]

(1. *College of Geographical Sciences*, *Changchun Normal University*, *Changchun* 130032, *China*; 2. *Northeast Institute of Geography and Agroecology*, *Chinese Academy of Science*, *Changchun* 130102, *China*)

Abstract: Algal blooms in lakes have become a common global environmental problem. Nowadays, remote sensing is widely used to monitor algal blooms in lakes due to the macroscopic, fast, real-time characteristics. However, it is often difficult to distinguish between algal blooms and aquatic vegetation due to their similar spectral characteristics. In this paper, we used modified vegetation presence frequency index (VPF) based on Moderate-resolution Imaging Spectroradiometer (MODIS) imagery to distinguish algal blooms from aquatic vegetation, and analyzed the spatial and temporal variations of algal blooms and aquatic vegetation from a phenological perspective for five large natural lakes with frequent algal bloom outbreaks in China from 2019 to 2020. We simplified the VPF method to make it with a higher spatial transferability so that it could be applied to other lakes in different climatic zones. Through accuracy validation, we found that the modified VPF method can effectively distinguish between algal blooms and aquatic vegetation, and the results vary from lake to lake. The highest accuracy of 97% was achieved in Hulun Lake, where the frequency of algal outbreaks is low and the extent of aquatic vegetation is stable, while the lowest accuracy of 76% was achieved in Dianchi Lake, which is rainy in summer and the lake is small. Analyses suggests that the time period when algal blooms occur most frequently might not coincide with that when they have the largest area. However, in most cases these two are close in terms of time period. The modified VPF method has a broad scope of application, is easy to implement, and has a high practical value. Furthermore, the method could be established using only a small amount of measured data, which is useful for water quality monitoring on large spatial scales.

Keywords: algal blooms; aquatic vegetation; modified vegetation presence frequency index (VPF); phenology; lake

Citation: PU Jing, SONG Kaishan, LIU Ge, WEN Zhidan, FANG Chong, HOU Junbing, LV Yunfeng, 2022. Differentiation of Algal Blooms and Aquatic Vegetation in Chinese Lakes Using Modified Vegetation Presence Frequency Index Method. *Chinese Geographical Science*, 32(5): 792−807. https://doi.org/10.1007/s11769-022-1301-5

1 Introduction

Algal blooms are harmful to the environment, they cause the deterioration of water quality, and the substances produced during algal blooms have a toxicological effect on aquatic organism and humans (Paerl, 2008; Hilborn et al., 2014; Wells et al., 2015; Kudela et al., 2017; Wells et al., 2020). Nowadays, algal blooms have become a common global environmental problem (Harke et al., 2016). Studies have showed that the aquatic vegetation played an important role in maintaining the balance of aquatic ecosystems (Blindow et al., 2002;

Received date: 2021-12-05; accepted date: 2022-05-08

Foundation item: Under the auspices of National Key Research and Development Project of China (No. 2021YFB3901101), National Natural Science Foundation of China (No. 41971322, 42071336, 42001311, 41730104), Jilin Provincial Science and Technology Development Project (No. 20180519021JH), Youth Innovation Promotion Association of Chinese Academy of Sciences (No. 2020234), China Postdoctoral Science Foundation (No. 2020M681057)

Corresponding author: LV Yunfeng. E-mail: lvyunfeng@ccsfu.edu.cn

Hughes et al., 2009; Zhao et al., 2012), they can promote nutrient cycling and effectively inhibit algal growth. The ecological effects of the aquatic vegetation and algal growth are quite different, and they often co-occur in the aquatic environment (Liu et al., 2013). Field surveys can effectively distinguish them, but these surveys are costly and time-consuming, and it difficult to realize the large-scale and long-term real-time monitoring. Remote sensing technology provides a new way to monitor the spatial and temporal characteristics of algal blooms in a large-scale and in real-time at much lower economic costs compared to field surveys (Gower et al., 2005; Chen and Quan, 2012; Stumpf et al., 2012; Klemas, 2013; Oyama et al., 2015; Wang et al., 2015; Yu et al., 2015; Zhang et al., 2015; Gorelick et al., 2017; Zhu et al., 2019; Coffer et al., 2020). Now, remote sensing images have been successfully adopted to monitor algal blooms in various lakes around the world, such as Erie Lake and Taihu Lake (Kahru et al., 2007; Hu et al., 2010; Wynne et al., 2010; Bresciani et al., 2011; Oyama et al., 2015; Palmer et al., 2015; Cao et al., 2016; Li et al., 2017; Fang et al., 2018) .

The commonly used remote sensing method for extracting algal blooms was based on the reflection peak signal of chlorophyll in the near-infrared, however, the spectral characteristics of algal blooms and aquatic plants are similar, this method can not differentiate aquatic plants from algal blooms (Ho et al., 2019; Feng et al., 2020). Although phycocyanin, a pigment unique to cyanobacteria, was successfully used to distinguish algal blooms from aquatic plants (Simis et al., 2005; Tyler et al., 2009; Dash et al., 2011), only a few satellite sensors can capture its band feature (620 nm), including the Oceansat-1 satellite Ocean Colour Monitor (OCM), Medium Resolution Imaging Spectrometer (MERIS), Sentinel-3 Ocean, and Land Colour Instrument (OLCI), and hyperspectral imagery (Liu et al., 2018). Researchers have attempted to differentiate algal blooms and aquatic plants using long time series data with low cost, such as Moderate Resolution Imaging Spectroradiometer (MODIS), Thematic Mapper (TM), *etc*. Oyama et al. (2015) combined the normalized difference water index (NDWI) and floating algae index (FAI) to construct a decision tree to discriminate between algal blooms and aquatic vegetation. However, this tree could not distinguish algal blooms from submerged vegetation (Oyama et al., 2015). The Cyanobacteria and Macrophytes Index (CMI) and FAI were combined to construct a decision tree to distinguish cyanobacteria blooms from aquatic vegetation in Taihu Lake. However, a priori knowledge was needed to distinguish between areas affected by algal bloom and areas frequently covered by aquatic vegetation (Liang and Yan, 2017). Zhu et al. (2018) developed a model for discriminating algal blooms from floating leaf vegetation by combining chlorophyll spectral indices and phycocyanin baselines. This study applied empirical measurements of surface reflectance spectra of Taihu Lake and used MERIS imagery to distinguish algal blooms from floating leaf vegetation. However, MERIS ceased to operate in April 2012 (Zhu et al., 2018). All models mentioned above require the support of measured hyperspectral data. They can only distinguish between some components of the aquatic vegetation and can not be directly applied to lakes across regions. Due to the complexity and uncertainty of the identification method, an empirical approach would be preferable to eliminate the aquatic vegetation growth area or remove the aquatic vegetation interference using methods such as eroding the vegetation signal close to the shore, especially in complex situations where emergent vegetation, submerged aquatic vegetation, and algal blooms coexist (Luo et al., 2017).

From the perspective of frequency analysis, we can distinguish between algal blooms and aquatic vegetation according to their spatial distribution at different times. Aquatic plants are always immobile on the water surface, while algal blooms drift on the lake surface. Since MODIS data can be obtained up to once a day for the same area, the revisit period is short and suitable for observing vegetation change over time. Therefore, MODIS data were selected as the data source in this study. The aims of this study were to: 1) distinguish algal blooms from aquatic vegetation using a modified VPF (vegetation presence fre-quency index) method; 2) monitor algal blooms in some large natural lakes with a high frequency of algal boom outbreaks in China based on MODIS data, and analyze the dynamic process of algal bloom formation and development; 3) determine the best conditions for the modified VPF method to distinguish between algal blooms and aquatic vegetation. This study attempts to distinguish between algal blooms and aquatic vegetation in lakes in different climatic zones of China using only a few field measure-

ments to demonstrate the spatial transferability of the method. The discussion of adaptability provides a reference for the subsequent wider application of the VPF method.

2 Materials and Methods

2.1 Study area

China is the third-largest country in the world, with 2921 naturally occurring lakes in China, accounting for ~0.9% of China's total land area (Ma et al., 2011; Song et al., 2021). Based on the basic characteristics of China's landscape and climate (Fig. 1) and their regional differences, there are five major lake regions, i.e., the Tibetan Plateau Lake Zone, Inner Mongolia-Xinjiang Lake Zone, Yunnan-Guizhou Plateau Lake Zone, Eastern Plain Lake Zone, and Northeast Plain and Mountain Lake Zone (Ma et al., 2011). Algal blooms can occur in most of these lake regions, except the Qinghai-Tibet Plateau region (due to less human activities) (Wang and Dou, 1998). According to the nutrient monitoring records of the Ministry of Ecology and Environment of the People's Republic of China in 2019, China's lakes and reservoirs with poor nutrient status, medium nutrient status, mild eutrophication, and moderate eutrophication accounted for 9.3%, 62.6%, 22.4%, and 5.6%, respectively (http://www.mee.gov.cn/hjzl/sthjzk/zghjzkgb/202006). Large natural lakes with a high frequency of algal boom outbreaks in China were selected for this study. These lakes were Taihu Lake, Hulun Lake, Chaohu Lake, Hongze Lake and Dianchi Lake (Fig. 1).

Chaohu Lake (30°34′N–32°12′N, 117°00′E–118°17′E) in the central Anhui Province has a subtropical climate and a water surface area of 573 km². It is the fifth-largest freshwater lake in China. The average water depth is 2.69 m, and the maximum depth is 3.77 m (Wang and Dou, 1998). Over the past few decades, industrialization and urbanization have intensified in the

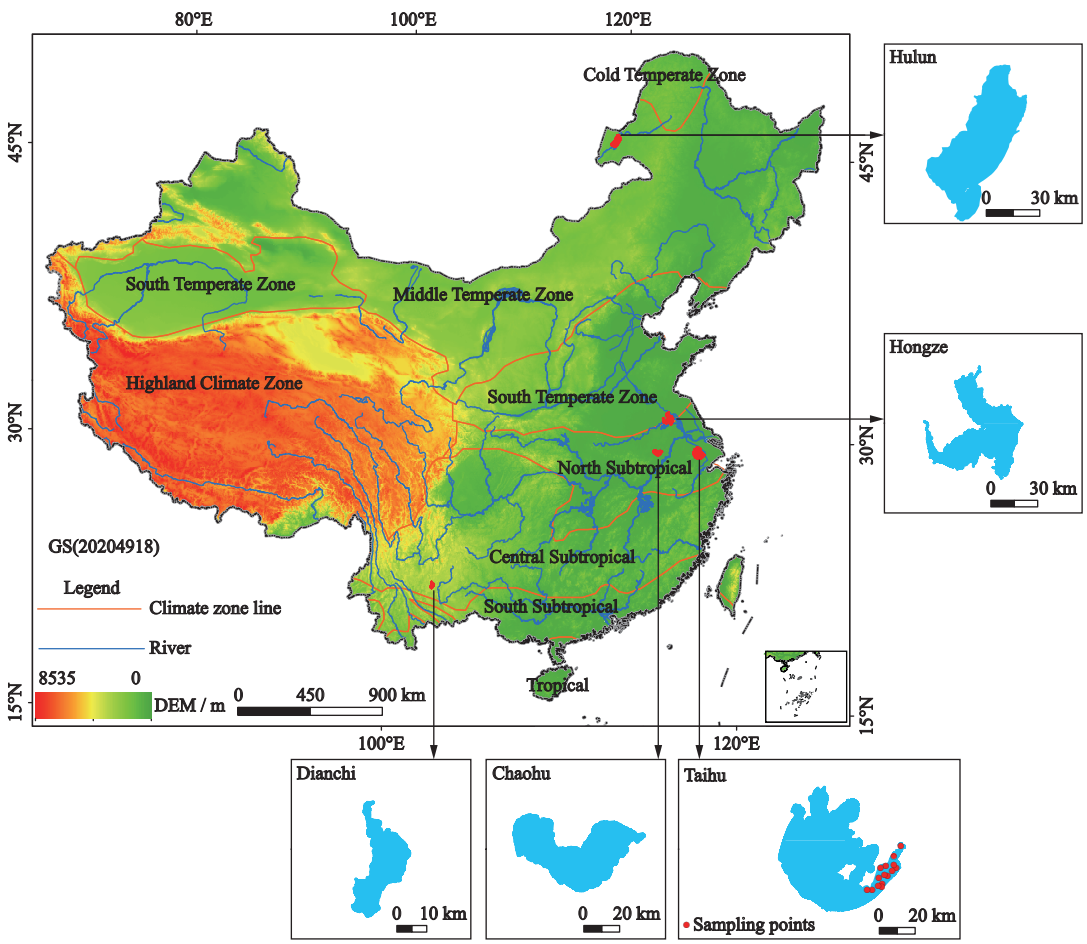

Fig. 1 Location of five study lakes in China

Basin of Chaohu Lake. Due to the massive discharge of urban sewage and agricultural runoff, Chaohu Lake has gradually changed from a clear water state with abundant aquatic vegetation to a turbid state with massive algal blooms, and eutrophication has gradually increased (Bao et al., 2021).

Dianchi Lake (24°40′N–25°02′N, 102°36′E–103°40′E) is a highland lake located in Kunming of Yunnan Province, with a subtropical climate. Dianchi Lake covers an area of 330 km^2 and has an average depth of 2.93 m and a maximum depth of 5.87 m (Wang and Dou, 1998). About 90% of Kunming's wastewater is released into the lake, causing severe eutrophication. Therefore, the lake experiences massive algal blooms every year and is considered one of the most eutrophic freshwater lakes in China (Huang et al., 2014; Cao et al., 2016).

Hulun Lake (48°43′N–49°20′N, 116°58′–117°48′E) is in the Hulun Buir grassland in the western part of the Greater Hinggan Mountains and the northeastern part of the Mongolian Plateau, which belongs to the temperate climate. It is the largest freshwater lake in the northern China, with a size of 2339 km², a maximum depth of 8.0 m, and an average depth of 5.7 m (Wang and Dou, 1998). In the last 20 yr, water levels in the northeast have declined, and the Xinkai River has become an inflowing river to Hulun Lake in recent years (Fang et al., 2019). This has created favorable conditions for algal blooms and a gradual increase in eutrophication.

Hongze Lake (33°06′N–33°40′N, 118°10′E–118°52′E), which has a southern temperate climate, is the fourth largest freshwater lake in China. It is also a typical large shallow lake with an area of 1805 km². The lake's average depth is 1.77 m, and its highest depth is 4.37 m (Wang and Dou, 1998). Its main water source is the Huaihe River. Due to the rapid renewal of the lake, algae are less likely to accumulate. As a result, the intensity and frequency of algal blooms are much lower than those in Taihu Lake (Huang et al., 2010).

Taihu Lake (30°55′N–31°32′N; 119°52′E–120°36′E) is in the Yangtze River Delta. The climate is characterized by a subtropical climate. It is the third-largest freshwater lake in China, with an area of 2338 km^2. Its maximum and average depths are 2.6 m and 1.9 m, respectively (Wang and Dou, 1998). The rapid economic growth, urbanization, and industrialization in the Taihu Lake Basin have also resulted in increasing domestic, industrial, and agricultural wastewater discharges. In addition, algal blooms have significantly increased in Taihu Lake in recent years. This severely threatens the safety of drinking water in the surrounding cities (Qin et al., 2007; Liang et al., 2017).

2.2 Field sampling data

Taihu Lake has the largest distribution of aquatic vegetation and algal blooms of the five lakes, so we carried out field sampling in Taihu Lake to aid our identification of algal blooms and aquatic vegetation in the images. During a field survey on May 6, 2020, aquatic vegetation was collected from 15 locations in Taihu Lake (Table S1), mainly concentrated in the East Taihu Lake area with dense aquatic vegetation. The location of each sampling point and the type of aquatic vegetation were recorded. The field data were used to distinguish between aquatic vegetation areas and non-aquatic areas. The distribution of the sampling sites in Taihu Lake is shown in Fig. 1.

2.3 Remote sensing data and processing

MODIS contains 36 spectral bands at moderate resolution levels (0.25 to 1.00 μm) and observes the Earth's surface every 1–2 d. MODIS product data images can be downloaded from NASA's EARTHDATA website (https://ladsweb.modaps.eosdis.nasa.gov/search/). The Level-2 Tiled surface reflectance data MYD09GA (500 m surface reflectance) from the Aqua satellite were selected for this study. The data have been calibrated and can be used without pre-processing steps.

Over 3500 images from 2019 to 2020 were downloaded, extracted, fused, and clipped according to visual interpretation methods, eliminating images that were heavily influenced by clouds, solar flares, and aerosols, leaving a total of 869 clipped, high-quality images of the five lakes (Table S2).

2.4 Methods

2.4.1 Modified VPF method

In the visual identification of algal blooms, asynchronous images are often used to exclude the possibility of false detections caused by aquatic vegetation. Algal blooms float with variable positions, whereas aquatic plants are rooted in the substrate, and their position is usually fixed (Luo et al., 2014; Song et al., 2021). We can therefore distinguish between algal blooms and

aquatic plants using an index of the frequency of vegetation signal occurrence.

Liu et al. (2015) first proposed the concept of the VPF in 2015 and implemented it to extract the aquatic vegetation of Taihu Lake. This study divided the growth period of the aquatic vegetation in Taihu Lake into three stages based on field data. It delineated VPF thresholds for different periods and also used water depth information to identify the growth range of aquatic vegetation. First, it is challenging to delineate the three stages of aquatic vegetation growth and set VPF thresholds for each stage without familiarity with a lake and sufficient field data. Second, water depth data for the whole lakes are usually not readily available. Due to the weak spatial transferability of the method, it is difficult to be used directly on other lakes.

In the present paper, Liu et al. (2015)'s method was improved, and our modified VPF method simplified the steps. The water surrounding the aquatic vegetation is usually of good quality and almost without algal blooms (Luo et al., 2014). Therefore, the maximum extent of aquatic vegetation was obtained only during the summer months when the area of aquatic vegetation was the largest, and the aquatic vegetation area was used as a mask to distinguish between aquatic vegetation and algal blooms. The specific steps are displayed in Fig. S1. We used the frequency distribution of the summer vegetation signal to obtain the maximum extent of aquatic vegetation and thus distinguish algal blooms and aquatic vegetation (Pu et al., 2022).

Although the location of aquatic plants is relatively stable over short periods, there are significant physical changes throughout the year and changes in their spatial distribution between years due to natural or human disturbances (Wang et al., 2019). In temperate and subtropical climates, plants thrive in summer and die off in winter. Therefore, they need to be analyzed on different time scales.

The FAI is a MODIS-based index for identifying algal blooms. The FAI was tested and reported to be suitable for stable extraction of algal bloom areas under relatively turbid conditions due to its low sensitivity to changes in some environmental conditions, such as aerosol thickness and solar flares (Hu, 2009). As the MYD09GA product used in this study has been calibrated to exclude atmospheric interference, the surface reflectance was used here instead of the Rayleigh-corrected reflectance in the original equation.

The FAI was calculated using the following equation:

$$FAI = (R_{nir} - R_{red} - (R_{swir} - R_{red})(\lambda_{nir} - \lambda_{red})/(\lambda_{swir} - \lambda_{red})) \quad (1)$$

where R_{nir}, R_{red}, and R_{swir} are the surface reflectance of the near-infrared, red and short-wave infrared bands, respectively. λ_{nir}, λ_{red}, and λ_{swir} are the central wavelengths of the near-infrared, red and short-wave infrared bands, respectively.

The vegetation presence frequency (VPF) of pixel j was calculated using Eq. (2). When the FAI value of pixel j of image i was greater than a set threshold and considered vegetation (including aquatic vegetation and algal blooms), pixel j entered the FAI calculation layer ($LFAI$) and was assigned a value of 1. Otherwise, it was assigned a value of 0. When there were n images in total, the VPF of pixel j was calculated as follows (Liu et al., 2015).

$$VPF(j) = \frac{\sum_{i=1}^{n} LFAI(j,i)}{n} \quad (2)$$

where VPF is the frequency of vegetation presence for pixel j in image i.

2.4.2 Setting of thresholds for the FAI and VPF

Hu et al. (2010) used an FAI threshold of –0.004 to distinguish algal blooms from non-algal blooms in Taihu Lake. Through field data validation, Liu et al. (2015) obtained an FAI threshold of –0.025 to identify vegetation signals (algae and aquatic plants). However, these thresholds are for Rayleigh-corrected reflectance data, and thresholds for surface reflectance data are different.

To obtain a suitable threshold, a total of 1796 reflection points, including vegetation (algae and aquatic plants) and water bodies, were extracted as sample data, their FAI values were entered into SPSS, and the best FAI classification threshold (i.e., 0.003) was obtained using the SPSS decision tree automatic classification function.

The threshold value for the VPF was determined by combining the results of the vegetation signal extracted by the FAI and the measured data provided in Table S1 for the discrimination of aquatic vegetation growth areas.

2.4.3 Verification methods

The high spatial variability of algal blooms makes it dif-

ficult to validate their accuracy, so we validate the accuracy of FAI extraction of vegetation signals (both algal blooms and aquatic vegetation) and the accuracy of aquatic vegetation extent to evaluate the accuracy of the method. In Google Earth imagery, areas of aquatic vegetation are apparent. Therefore, we used Google Earth for accuracy verification. Google Earth images of the same period as the vegetation boundary extraction results were selected for accuracy verification. Sampling points were evenly distributed within the maximum extent of aquatic vegetation, and the spacing between sampling points via ArcGIS's fishing net tool varied depending on the lake. We regarded 100–200 validation points as appropriate for each lake. Fewer validation points should not be representative, while more validation points would not be feasible. The accuracy was verified based on the date the image was taken in Google Earth and the feature type. For areas where images were sparse and no suitable contemporaneous images were available on Google Earth, images from the most recent period were used for verification. The precision P was calculated as follows

$$P = PT / (PT + PF) \tag{3}$$

where P is the precision obtained by validation. It was verified that PT was the correct point and PF was the wrong point.

3 Results

3.1 Distinguishing the aquatic vegetation from algal blooms

The results of FAI extraction for 2019 and 2020 showed that neither aquatic vegetation nor algal blooms were apparent in Taihu Lake, Hongze Lake, and Chaohu Lake in December and January. The plant area gradually expanded from February to May. From June to October, the area of aquatic plants reached the maximum level but was relatively stable from July to September. In November, the area decreased rapidly. Hulun Lake has a long freezing period due to its higher latitude, with May–September being the warmer period of the year. Plants start to grow when the lake thaws in May, and the growth area stabilizes by July, with July–September being the peak of plant growth and algal blooms. Dianchi Lake is located at a lower latitude and has a warmer climate. High-quality images were available for summer due to the high precipitation. The images showed that the area of aquatic vegetation growth was relatively small from November to February, with marginal changes in area during the rest of the year. From March to October, the area of aquatic vegetation was stable, while the occurrence of algal blooms was high. To effectively distinguish between aquatic vegetation and algal blooms, this study focused on the peak period when aquatic vegetation and algal blooms thrive. We set the VPF time frame for Taihu Lake, Hongze Lake, Chaohu Lake, and Hulun Lake from July to September and for Dianchi Lake from March to October.

Fig. S2 shows the FAI extraction results for Taihu Lake from January to December in 2020, with one selected scene per month. It shows how the vegetation signal changed in Taihu Lake, i.e., almost no aquatic vegetation occurred from December to April, vegetation started to grow in May, the vegetated area was stable in July–September and began to decline in October.

Based on the times selected above, we superimposed the LFAI for the five lakes for that period to calculate the VPF (Fig. 2). Red denotes a high occurrence of the vegetation signal, meaning that it had a high probability of being aquatic vegetation. Green denotes a less frequent vegetation signal.

Aquatic vegetation can purify water and inhibit algal growth. Accordingly, its surroundings generally have good water quality and little eutrophication. The vegetation presence frequency index VPF ranges from 0 to 1 and should be greater than 0.5 for aquatic plants with a fixed position. Comparing different thresholds, we noticed that when the threshold value was < 0.7, some areas covered by algal blooms for a long time were mistaken for aquatic vegetation (e.g., Zhushan Bay and Meiliang Bay in the northern part of Taihu Lake, where severe eutrophication led to frequent algal blooms). Some areas with submerged plants (e.g., Xukou Bay and East Taihu Lake in Taihu Lake) were mistaken for algal blooms if the threshold value was > 0.8. The field data in Table S1 were combined with the VPF in Fig. 2 to select the most appropriate VPF threshold. We deduced through repeated tests that the distribution of algal blooms and aquatic vegetation matched the field situation and achieved the best differentiation by setting the threshold value to 0.75.

With a VPF greater than 0.75, we extracted the boundaries of the aquatic vegetation. This was then used

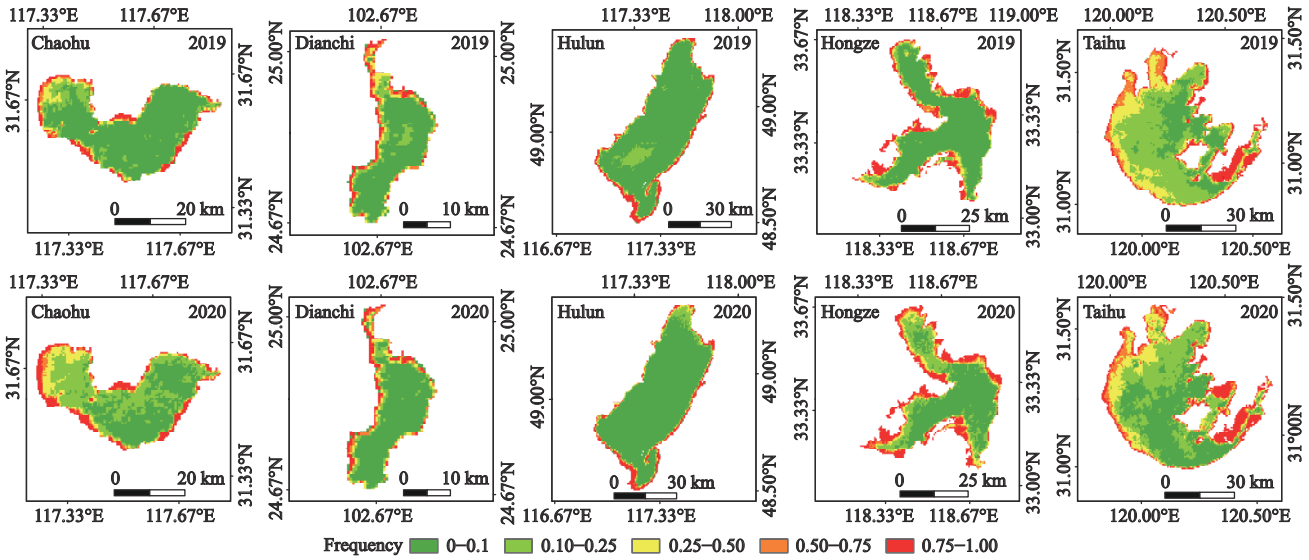

Fig. 2 VPF (vegetation presence frequency) distribution in summer of 2019 and 2020 for large lakes in China

to crop the vegetation signal extracted by the FAI to obtain the area of algal bloom. The distributions of algal blooms and aquatic vegetation in the studied lakes in summer are presented in Fig. 3.

3.2 Validation results

3.2.1 Precision of FAI thresholds

An optimal classification FAI threshold of 0.003 was obtained by automatic SPSS decision tree classification. We extracted 908 points (including 511 vegetation and 397 water body points without macrophytes and algae) of reflectance for validation, and the overall classification accuracy was 89.10% (Table 1).

3.2.2 Precision of vegetation boundaries

The accuracy of the obtained aquatic vegetation areas was verified using homogenous spatial distribution of sampling points. The number of validation points for the five lakes, and the accuracy of validation are shown in Table 2.

Accuracies were higher than 76% across lakes, and Hulun Lake had the highest accuracy. The distribution of the validation points and the respective validation results are shown in Fig. 4.

3.3 Temporal changes in algal bloom distribution

The area of the algal blooms was obtained by clipping the maximum extent of aquatic vegetation extracted by the VPF with the vegetation extent extracted by the FAI, and an area greater than 0 was considered to have an algal bloom. Fig. 5a indicated that in 2019 and 2020 algal blooms in Chaohu Lake occurred mainly from May to November. Small algal blooms could occur in January and February. In Hongze Lake, algal blooms mostly appeared in August and September. In Dianchi Lake, algal blooms frequently occurred from October to December, but analyses suggested that this might have been related to the low availability of high-quality images in summer. Algal blooms in Hulun Lake were concentrated in July–August.

To obtain the true frequency of algal outbreaks in different months, we divided the number of algal blooms observed per month by the number of images available for each month. Fig. 5b shows the frequency of algal blooms for each lake over the two years. Chaohu Lake had the highest frequency of algal blooms from July–September, with minor occurrences in January and February. Dianchi Lake had the highest frequency of algal outbreaks in August and blooms occurred relatively infrequently from December to February. Hulun Lake experienced the highest frequency of algal blooms in August due to the relatively short summer, i.e., algal blooms occurred during the peak temperature between July and September. In Hongze Lake, algal blooms frequently occurred from August to September, with a small number of algal blooms from March to April. In Taihu Lake, algal blooms were frequently found throughout the year, with a first peak appearing between April and May, after which they continued until November. In the worst cases, Dianchi, Taihu, and Chaohu, algal blooms occurred almost all year round, with a

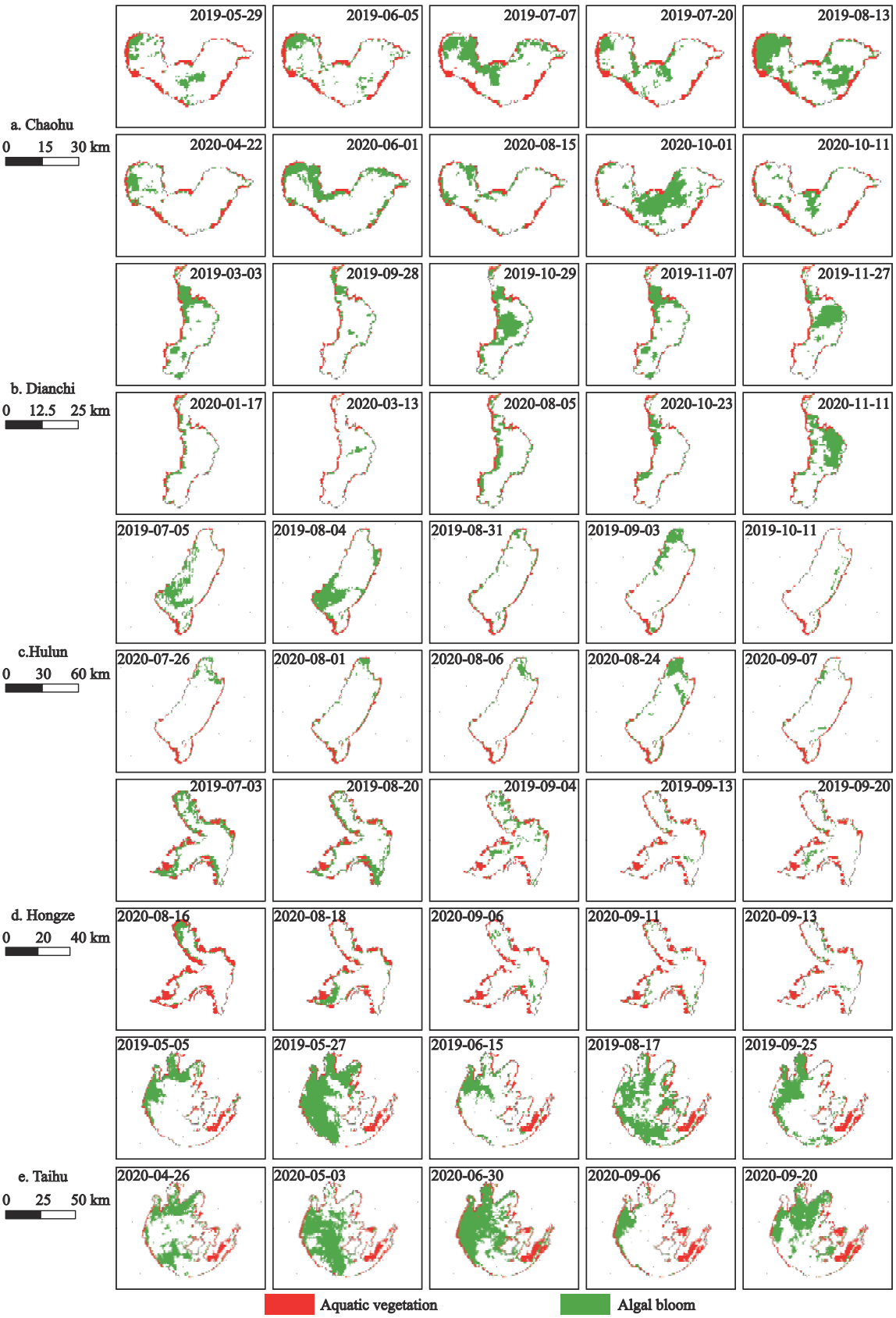

Fig. 3 Distribution of algal blooms and aquatic vegetation in the studied lakes identified by the modified VPF method in 2019 and 2020

Table 1 Confusion matrix to distinguish vegetation from water bodies

Type	Vegetation	Water bodies	Total	Producer accuracy / %	User accuracy / %	Overall accuracy / %
Vegetation	397	99	496	80.04	100.00	
Water bodies	0	412	412	100.00	80.63	
Total	397	511	908			89.10

Table 2 Validation points number and the calculated accuracy results for five large lakes in China

Year	Chaohu Lake		Dianchi Lake		Hulun Lake		Hongze Lake		Taihu Lake	
	T	F	T	F	T	F	T	F	T	F
2019	47	21	86	28	25	1	98	16	95	22
2020	60	9	94	27	130	3	100	19	12	9
Total	107	30	180	55	155	4	198	35	107	31
Precision / %	78.10		76.60		97.48		84.98		77.54	

Notes: T is true, and F is false

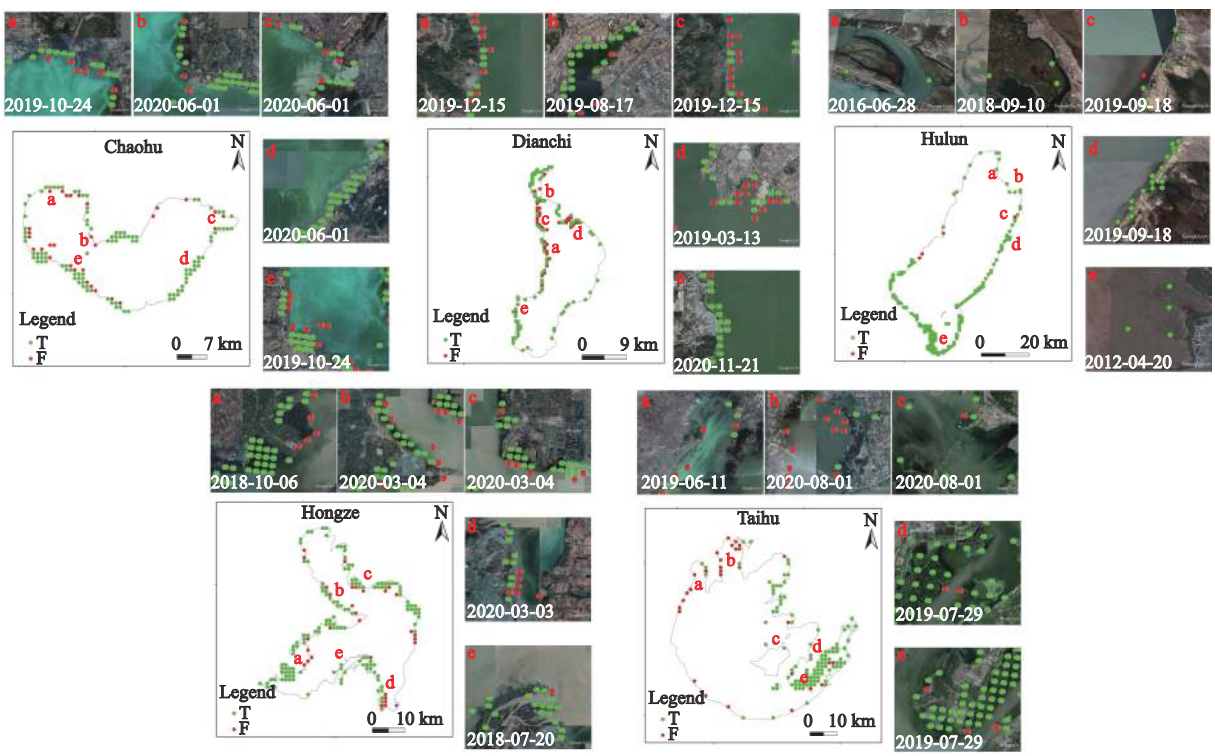

Fig. 4 Distribution of validation points and validation results for five large lakes in China in 2019 and 2020. T is true, and F is false

shorter dormant period in winter, i.e., there was a vicious cycle of algal blooms, with severe eutrophication leading to algal blooms, resulting in deterioration of water quality, which caused more frequent algal blooms in turn . In contrast, the dormant periods of algal blooms were longer under the relatively good conditions of Hongze Lake and Hulun Lake.

3.4 Variation in algal bloom occurrence area

Due to limited images of Taihu Lake and Dianchi Lake for the summer of 2020, this study used the 2019 data for area calculations to obtain a more comprehensive picture of the changes in aquatic vegetation and algal bloom areas.

The area of the extracted vegetation signal was calcu-

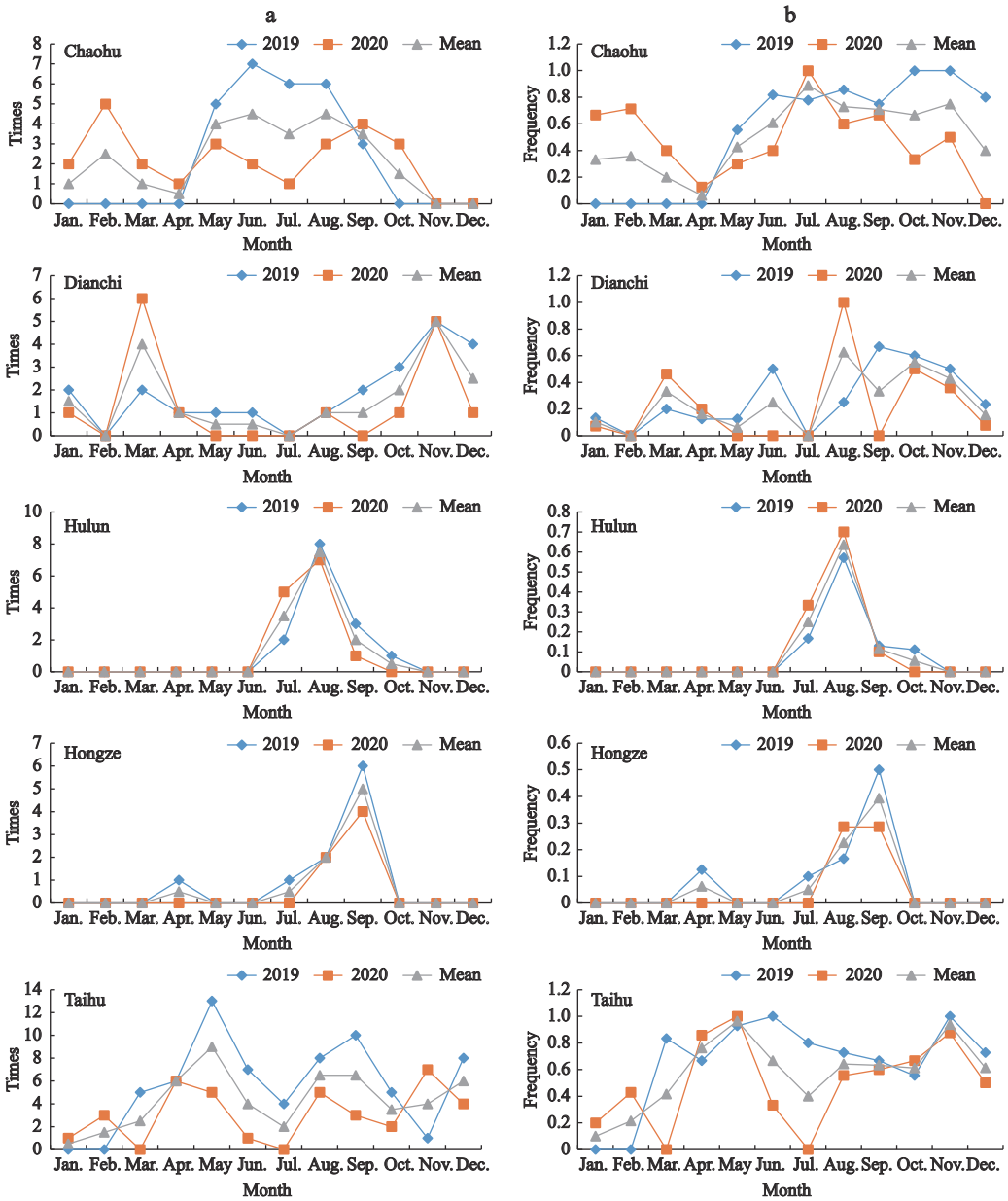

Fig. 5 Times (a) and frequency (b) of observed algal blooms per month in 2019, 2020, and two-year average for five large lakes in China. Frequency is the ratio between the times of algal blooms observed per month and the number of MODIS images available for each month

lated and then counted separately according to the classification results. The aquatic vegetation area was divided by the maximum aquatic vegetation area to obtain the proportion between aquatic vegetation and total aquatic vegetation area at different times in 2019 (Fig. 6). The algal bloom area was divided by the whole lake area to obtain the proportion between algal bloom and whole lake area at different times in 2019 (Fig. 7). The final variation in the areas of aquatic vegetation and algal blooms over time was obtained separately. Aquatic vegetation growth and the development of algal blooms were revealed. The areas of aquatic vegetation in Chaohu Lake, Hulun Lake, Hongze Lake, and Taihu Lake peaked and stabilized between July and September. In contrast, the aquatic vegetation area in the warmer Dianchi Lake did not vary significantly over time, but a downward trend was apparent in December and January–February. The algal bloom areas in Chaohu Lake, Dianchi Lake, Hulun Lake, Hongze Lake, and Taihu Lake peaked in July–October, June–October, August, July–September, and August–October, respectively.

Our analysis of the relationship between the area of

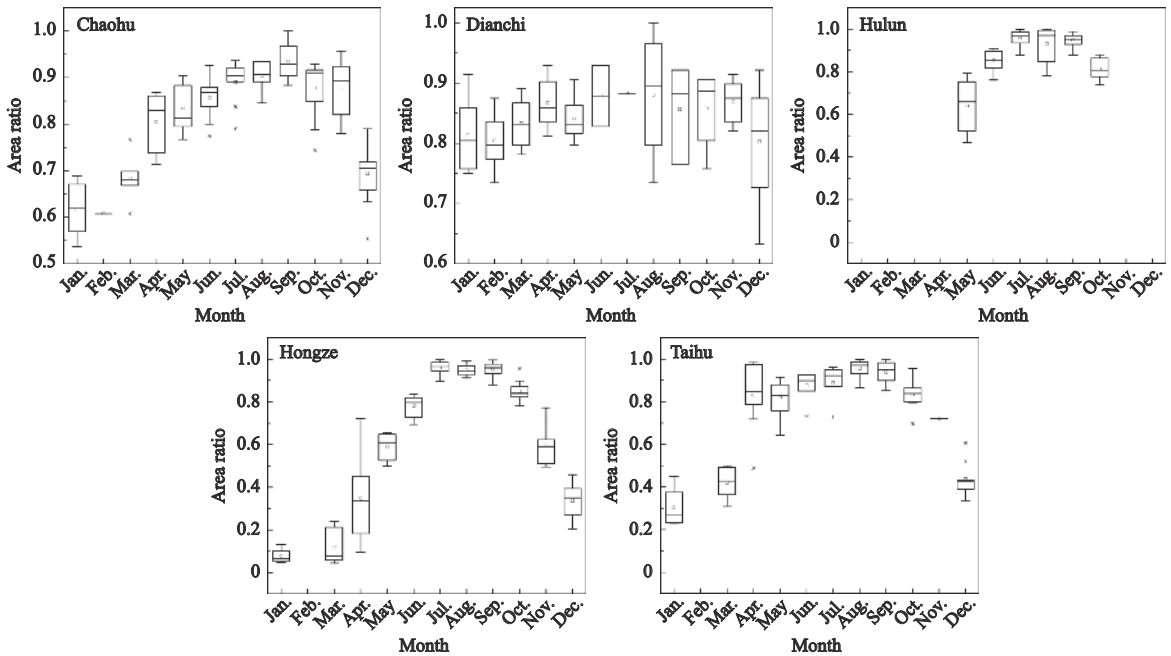

Fig. 6 Changes in aquatic vegetation area of the study lakes in China in 2019. Area ratio is the area of the aquatic vegetation divided by the maximum area of aquatic vegetation

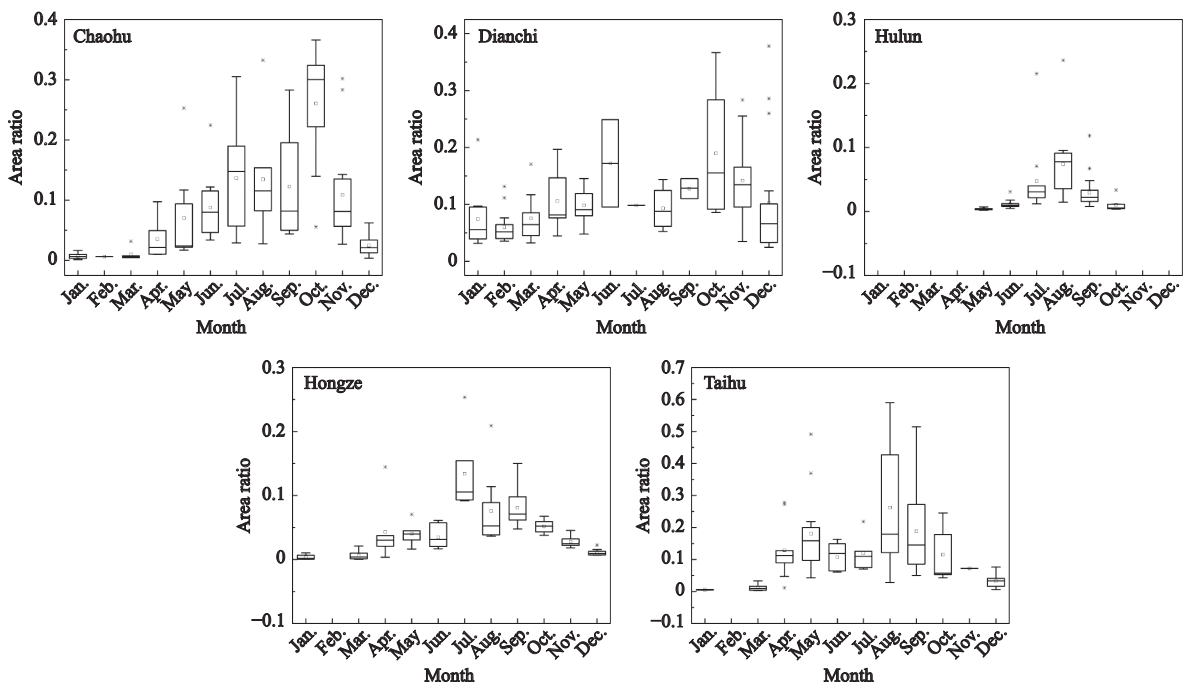

Fig. 7 Changes in algal bloom areas of the study lakes in China in 2019. Area ratio is the area of algal blooms divided by the area of the correspongding lake

algal bloom occurrence and the time of year suggested that the period when algal blooms occurred most frequently might not coincide with the period of their largest extension. However, in most cases, the two periods were close.

4 Discussion

4.1 Advantages and Limitations of the modified VPF method

Compared to other methods for differentiating between

algal blooms and aquatic vegetation using remote sensing imagery, our method does not require in situ-measured reflectance spectra and uses very little field data. It is not limited to a single lake or a class of lakes but worked well for five lakes with different geographical, climatic, and environmental conditions. Our method requires few in situ data, is easy to operate, has broad applicability, and is spatially transferable. In contrast to field surveys, MODIS imagery is sampled once a day in clear weather, which is almost impossible to achieve manually. The method used in this paper enables the dynamic analysis of the occurrence and spatial changes of algal blooms.

With a low spatial resolution of 500 m, MODIS imagery might not reflect detailed features and could only be used to monitor large lakes, i.e., it is less applicable for small lakes. Although the Landsat series of images has a high spatial resolution, the revisit period is long. Besides, the climate in China is characterized by frequent rain in summer. Thus the available images might not be sufficient to calculate the vegetation presence frequency. Moreover, low resolution increases the proportion of mixed pixels, and the accuracy of differentiation is reduced. For areas where the aquatic vegetation is relatively sparse or algal blooms are insignificant, blooms are challenging to detect using MODIS imagery.

The validation data in this study had some limitations. Only a small amount of field data was available for Taihu Lake. At the same time, the other four lakes had only limited information on algal blooms and aquatic vegetation from published papers. There was, therefore, some subjectivity. The data for the accuracy validation were also extracted from Google Earth maps. Although the maps' clarity can help identify areas of aquatic vegetation growth, only a few days of data was the maximum found for each lake for accuracy evaluation due to a limited number of highly legible maps.

Furthermore, the location of phytoplankton is variable. Hence the method introduced here might have misidentified them as algal blooms and caused errors (Palmer et al., 2015). Similarly, if an area is covered with algal blooms for a long time, it can be mistaken for aquatic vegetation. False extraction of turbid water bodies might occur when using the FAI to extract vegetation signals in highly turbid water bodies. For example, turbid water bodies were mistaken for vegetation in three images of Hulun Lake in September 2019 and October 2020 each, as well as in five images of Hongze Lake (Hu, 2009).

4.2 Compare to previous researches

4.2.1 The temporal variation of algal blooms

Chaohu Lake: Ma et al. (2021) reported that algal blooms in Chaohu Lake mainly occurred between May and November. The highest frequency of algal blooms in the northwestern section of Chaohu Lake occurred in October, and the highest frequency of blooms in the eastern section of Chaohu Lake in June. In this paper, algal blooms occurred throughout the year in Chaohu Lake, with a low frequency between December and March, the lowest frequency in April, and a peak between May and November, which is consistent with the temporal pattern of algal blooms reported by Ma et al. (2021). Dianchi Lake: Jing et al. (2019) suggested that algal blooms in Dianchi Lake occurred from late February to early the following year and lasted for a long time. The maximum occurrence of algal blooms happened in July and November . In this paper, the algal blooms also occurred in January–February, and March–December. Consistent with Jing et al. (2019), a double-peak trend was observed in August and October–November. Hongze Lake : Ren et al. (2014) found that algal blooms in Hongze Lake usually emerged in April–May, increased sharply in July, and lasted for 3–4 months. This study is highly consistent with the pattern observed in the present study, i.e., algal blooms appeared in April–May, increased rapidly in frequency in July, and peaked in August. Hulun Lake: Fang et al. (2019) indicated that algal blooms in Hulun Lake mainly occurred in August, followed by July and September, consistent with the temporal variation of the same lake in this paper. Taihu Lake: Zhu et al. (2018) showed that Taihu Lake algal blooms mainly occurred from May to October. In this paper, we found that Taihu Lake experienced algal blooms almost all year round, with a high frequency of occurrence after May and a low frequency after October.

4.2.2 The spatial variation of algal blooms

After removing the disturbance of aquatic vegetation, all FAI layers with algal bloom images were superimposed and then divided by the number of images to obtain the probability of the bloom appearing in different areas when it occurred. The locations of all algal blooms during the year and their frequency distribution are presen-

ted in Fig. 8.

Table 3 lists the spatial distribution of algal bloom occurrence in the five studied lakes according to other studies in recent years. Comparing Table 3 with Fig. 8, we found that this study's spatial distribution pattern of algal blooms is consistent with the results of other related studies. Thus, the spatial and temporal distribution pattern of algal blooms derived in this study is stable and reliable, reflecting the spatial and temporal variation pattern of algal blooms.

4.2.3 Implications

This study distinguished between algal blooms and aquatic vegetation in all five lakes we studied in different climatic zones. However, there were differences in accuracy between the different lakes, with the lowest accuracy for Dianchi (76%) and the highest for Hulun Lake (97%). Analyzing the reasons for the differences in accuracy will help us determine the method's applicability.

Compared to other lakes, identifications in Dianchi Lake had lower accuracy. However, Dianchi Lake is small. When using MODIS images to extract vegetation information, the border areas of aquatic vegetation could appear as mixed pixels due to the low resolution of the images, and the proportion of mixed pixels is greater in smaller lakes. Moreover, Dianchi is on the Yunnan-Guizhou Plateau, where the climate is cloudy and rainy in summer. Accordingly, image availability in summer is very limited. Images were selected from spring, summer, and autumn for the VPF calculation. The area of aquatic vegetation in spring and autumn was not the maximum extent of aquatic vegetation. Therefore, there was an under extraction of the maximum extent of aquatic vegetation.

The accuracy of Dianchi Lake, Taihu Lake, and Chaohu Lake—where algal blooms are more common—was low compared to Hulun Lake. Misclassified points in Taihu Lake were mainly concentrated in Zhushan Bay, Meiliang Bay, and the western shore with open water. In contrast, the wrong points in Dianchi

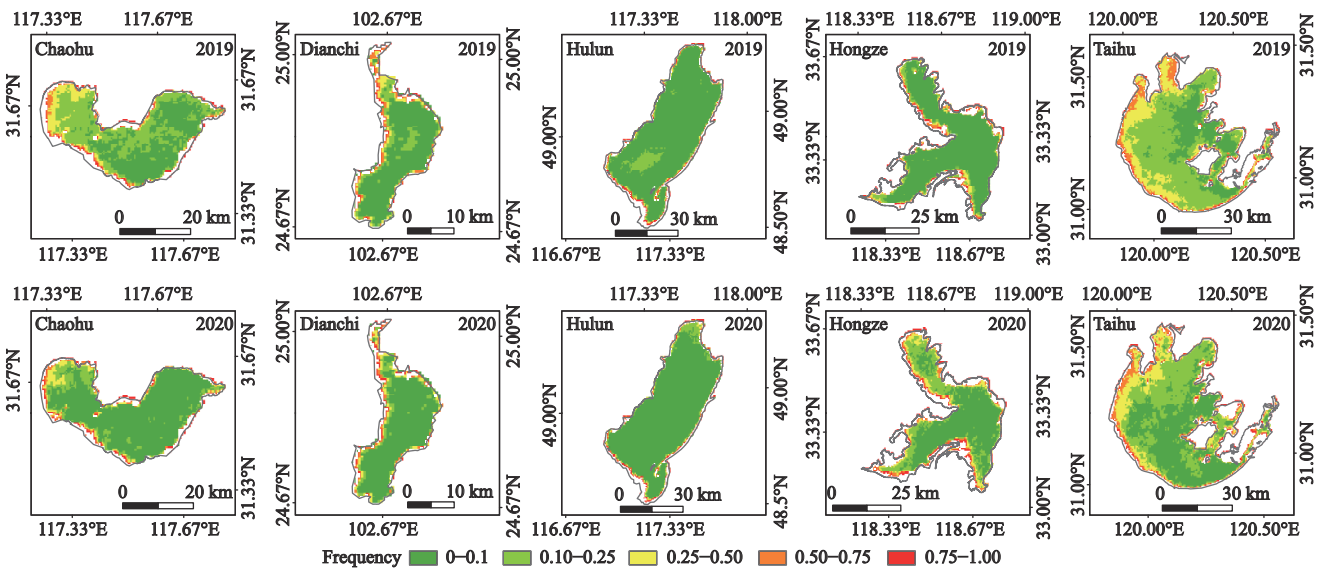

Fig. 8 Frequency of occurrence of algal blooms in different lakes in China in 2019 and 2020

Table 3 Frequency of algal blooms at different locations according to other studies for Lakes

Lake	Frequency of algal blooms at different locations	References
Chaohu Lake	More frequent in the west than in the centre and east	Zhang et al., 2015
Dianchi Lake	High in the northern section and low in the southern section, high at the edge of the lake and low in the centre	Jing et al., 2019
Hulun Lake	Concentrated at the border	Fang et al., 2019
Hongze Lake	Mainly in the western section of the lake, which is significantly higher than in the eastern section	Ren et al., 2014
Taihu Lake	The highest in Northwest Lake and Meiliang Bay, followed by Zhushan Bay, Gonghu Bay, Central Lake and Southwest Lake, and the lowest in East Lake	Hu et al., 2010; Zhang et al., 2020

Lake were mainly concentrated in the northern coastal area of the lake. The misclassified points in Chaohu Lake were on the western shoreline. All misclassified points were mainly in areas covered by algal blooms for a long time (Fig. 4) (Zhang et al., 2015; Shi et al., 2017; Jing et al., 2019). Checking the images of Hongze Lake on August 16 and 18, 2020, some submerged vegetation was classified as algal blooms in the northern and western parts of the lake. However, a small area of aquatic vegetation was also classified as an algal bloom in Xukou Bay in Taihu Lake. This occurred because Hongze Lake had a large area of submerged vegetation in the northern and western parts of the lake (Xia et al., 2011), and the aquatic vegetation in Xukou Bay was also dominated by submerged vegetation (Luo et al., 2017). Submerged vegetation is not easily observed in remote sensing imagery. Therefore the VPF values in the areas where submerged vegetation is distributed are low and mistaken for algal blooms. Also, misclassified points were mainly distributed close to the aquatic vegetation around the lake, and the analysis suggested that mixed image elements could drive the error.

Our analysis indicated that the lower the frequency of algal blooms, the smaller the VPF value of the algal bloom area, and the less likely it was mistaken for aquatic vegetation in the frequency calculation and, thus, the more accurate the classification of the aquatic vegetation area. The more stable the extent of aquatic vegetation, the higher the VPF value of the extent of aquatic vegetation, such as in Hulun Lake, and the more accurate the identification. The larger the lake area, the fewer mixed image elements, and the more accurate the identification. The modified VPF method has a wide range of applications, but its accuracy varies from lake to lake, and the best identification results can be achieved when the lake is large, the frequency of algal blooms is not particularly high, sufficient images are available in summer and the extent of aquatic vegetation is relatively stable.

5 Conclusions

In this study, we analyzed the spatial and temporal variations of algal blooms and aquatic vegetation in five large natural lakes in China from a phenological perspective with frequent algal bloom outbreaks using a modified VPF method to distinguish between algal blooms and aquatic vegetation. We implemented the distinguishing between algal blooms and aquatic vegetation by obtained the maximum extent of aquatic vegetation with the accuracy of 76%–97%. The modified VPF method showed a higher spatial transferability and was successfully applied to lakes in different climatic zones with the highest accuracy of 97% in Hulun Lake. It can effectively distinguish between algal blooms and aquatic vegetation in five studies lakes, and based on the results, we found that the time was not matched between the maximum occurrence frequency and the largest area of algal blooms.

Overall, the study helps us to understand the spatial and temporal variation in the occurrence of algal blooms on a larger scale through a proposed modified VPF method, allowing us to respond immediately to adverse environmental impacts and prevent socio-economic damage caused by algal blooms. Based on the spatial transferability and low dependence on field data of the method, the study provides the theoretical and technological support for large-scale algal bloom monitoring that is of practical relevance to water environment management and monitoring departments.

Appendix

Tables S1, S2 and Figs. S1, S2 could be found in the corresponding article at http://egeoscien.neigae.ac.cn/article/2022/5.

References

Bao H F, Li Y W, Diao X J et al., 2021. Effects of algal bloom (AB) on sediment microorganisms with special functions at different AB stages in Chaohu Lake. *Water Science & Technology*, 83(5): 1130–1140. doi: 10.2166/wst.2021.009

Blindow I, Hargeby A, Andersson G, 2002. Seasonal changes of mechanisms maintaining clear water in a shallow lake with abundant *Chara* vegetation. *Aquatic Botany*, 72(3–4): 315–334. doi: 10.1016/s0304-3770(01)00208-x

Bresciani M, Giardino C, Bartoli M et al., 2011. Recognizing harmful algal bloom based on remote sensing reflectance band ratio. *Journal of Applied Remote Sensing*, 5(1): 053556. doi: 10.1117/1.3630218

Cao X, Wang Y Q, He J et al., 2016. Phosphorus mobility among sediments, water and cyanobacteria enhanced by cyanobacteria blooms in eutrophic Lake Dianchi. *Environmental Pollution*, 219: 580–587. doi: 10.1016/j.envpol.2016.06.017

Chen J, Quan W T, 2012. Using landsat/TM imagery to estimate nitrogen and phosphorus concentration in Taihu Lake, China.

IEEE Journal of Selected Topics in Applied Earth Observations and Remote Sensing, 5(1): 273–280. doi: 10.1109/jstars.2011.2174339

Coffer M M, Schaeffer B A, Darling J A et al., 2020. Quantifying national and regional cyanobacterial occurrence in US lakes using satellite remote sensing. *Ecological Indicators*, 111: 105976. doi: 10.1016/j.ecolind.2019.105976

Dash P, Walker N D, Mishra D R et al., 2011. Estimation of cyanobacterial pigments in a freshwater lake using OCM satellite data. *Remote Sensing of Environment*, 115(12): 3409–3423. doi: 10.1016/j.rse.2011.08.004

Fang C, Song K S, Li L et al., 2018. Spatial variability and temporal dynamics of HABs in Northeast China. *Ecological Indicators*, 90: 280–294. doi: 10.1016/j.ecolind.2018.03.006

Fang C, Song K S, Shang Y X et al., 2019. Remote sensing of harmful algal blooms variability for Lake Hulun using adjusted FAI (AFAI) algorithm. *Journal of Environmental Informatics*, 34(2): 108–122. doi: 10.3808/jei.201700385

Feng L, Hou X J, Liu J G et al. , 2020. Unrealistic phytoplankton bloom trends in global lakes derived from Landsat measurements.https://doi.org/10.31223/osf.io/2wxnt.

Gorelick N, Hancher M, Dixon M et al., 2017. Google earth engine: planetary-scale geospatial analysis for everyone. *Remote Sensing of Environment*, 202: 18–27. doi: 10.1016/j.rse.2017.06.031

Gower J, King S, Borstad G et al., 2005. Detection of intense plankton blooms using the 709 nm band of the MERIS imaging spectrometer. *International Journal of Remote Sensing*, 26(9): 2005–2012. doi: 10.1080/01431160500075857

Harke M J, Steffen M M, Gobler C J et al., 2016. A review of the global ecology, genomics, and biogeography of the toxic cyanobacterium, *Microcystis* spp. *Harmful Algae*, 54: 4–20. doi: 10.1016/j.hal.2015.12.007

Hilborn E D, Roberts V A, Backer L et al., 2014. Algal bloom-associated disease outbreaks among users of freshwater lakes - United States, 2009−2010. *Morbidity and Mortality Weekly Report*, 63(1): 11–15.

Ho J C, Michalak A M, Pahlevan N, 2019. Widespread global increase in intense lake phytoplankton blooms since the 1980s. *Nature*, 574(7780): 667–670. doi: 10.1038/s41586-019-1648-7

Hu C M, 2009. A novel ocean color index to detect floating algae in the global oceans. *Remote Sensing of Environment*, 113(10): 2118–2129. doi: 10.1016/j.rse.2009.05.012

Hu C M, Lee Z P, Ma R H et al., 2010. Moderate resolution imaging spectroradiometer (MODIS) observations of cyanobacteria blooms in Taihu Lake, China. *Journal of Geophysical Research:Oceans*, 115(C4): C04002. doi: 10.1029/2009jc005511

Huang C C, Wang X L, Yang H et al., 2014. Satellite data regarding the eutrophication response to human activities in the plateau Lake Dianchi in China from 1974 to 2009. *Science of the Total Environment*, 485–486: 1–11. doi: 10.1016/j.scitotenv.2014.03.031

Huang L, Sun K, Ban J et al., 2010. Public perception of blue-algae bloom risk in Hongze Lake of China. *Environmental Management*, 45(5): 1065–1075. doi: 10.1007/s00267-010-9480-8

Hughes A R, Williams S L, Duarte C M et al., 2009. Associations of concern: declining seagrasses and threatened dependent species. *Frontiers in Ecology and the Environment*, 7(5): 242–246. doi: 10.1890/080041

Jing Y Y, Zhang Y C, Hu M Q et al., 2019. MODIS-satellite-based analysis of long-term temporal-spatial dynamics and drivers of algal blooms in a plateau Lake Dianchi, China. *Remote Sensing*, 11(21): 2582. doi: 10.3390/rs11212582

Kahru M, Savchuk O P, Elmgren R, 2007. Satellite measurements of cyanobacterial bloom frequency in the Baltic Sea: interannual and spatial variability. *Marine Ecology Progress Series*, 343: 15–23. doi: 10.3354/meps06943

Klemas V, 2013. Remote sensing of emergent and submerged wetlands: an overview. *International Journal of Remote Sensing*, 34(18): 6286–6320. doi: 10.1080/01431161.2013.800656

Kudela R M, Berdalet E, Enevoldsen H et al., 2017. GEOHAB the global ecology and oceanography of harmful algal blooms program: motivation, goals, and legacy. *Oceanography*, 30(1): 12–21. doi: 10.5670/oceanog.2017.106

Li J, Zhang Y C, Ma R H et al., 2017. Satellite-based estimation of column-integrated algal biomass in nonalgae bloom conditions: a case study of Lake Chaohu, China. *IEEE Journal of Selected Topics in Applied Earth Observations and Remote Sensing*, 10(2): 450–462. doi: 10.1109/jstars.2016.2601083

Liang K, Yan G Z, 2017. Application of landsat imagery to investigate lake area variations and relict gull habitat in Hongjian Lake, Ordos Plateau, China. *Remote Sensing*, 9(10): 1019. doi: 10.3390/rs9101019

Liang Q C, Zhang Y C, Ma R H et al., 2017. A MODIS-based novel method to distinguish surface cyanobacterial scums and aquatic macrophytes in Lake Taihu. *Remote Sensing*, 9(2): 133. doi: 10.3390/rs9020133

Liu G, Simis S G H, Li L et al., 2018. A four-band semi-analytical model for estimating phycocyanin in inland waters from simulated MERIS and OLCI data. *IEEE Transactions on Geoscience and Remote Sensing*, 56(3): 1374–1385. doi: 10.1109/tgrs.2017.2761996

Liu X H, Zhang Y L, Yin Y et al., 2013. Wind and submerged aquatic vegetation influence bio-optical properties in large shallow Lake Taihu, China. *Journal of Geophysical Research: Biogeosciences*, 118(2): 713–727. doi: 10.1002/jgrg.20054

Liu X H, Zhang Y L, Shi K et al., 2015. Mapping aquatic vegetation in a large, shallow eutrophic lake: a frequency-based approach using multiple years of MODIS data. *Remote Sensing*, 7(8): 10295–10320. doi: 10.3390/rs70810295

Luo J H, Ma R H, Duan H T et al., 2014. A new method for modifying thresholds in the classification of tree models for mapping aquatic vegetation in taihu lake with satellite images. *Remote Sensing*, 6(8): 7442–7462. doi: 10.3390/rs6087442

Luo J H, Duan H T, Ma R H et al., 2017. Mapping species of submerged aquatic vegetation with multi-seasonal satellite images and considering life history information. *International Journal of Applied Earth Observation and Geoinformation*, 57: 154–165. doi: 10.1016/j.jag.2016.11.007

Ma J Y, Jin S G, Li J et al., 2021. Spatio-temporal variations and driving forces of harmful algal blooms in Chaohu Lake: a multi-source remote sensing approach. *Remote Sensing*, 13(3): 427. doi: 10.3390/rs13030427

Ma Ronghua, Yang Guishan, Duan Hongtao et al., 2011. China's

lakes at present: number, area and spatial distribution. *Science China Earth Sciences*, 54(2): 283–289. doi: 10.1007/s11430-010-4052-6

Oyama Y, Matsushita B, Fukushima T, 2015. Distinguishing surface cyanobacterial blooms and aquatic macrophytes using Landsat/TM and ETM + shortwave infrared bands. *Remote Sensing of Environment*, 157: 35–47. doi: 10.1016/j.rse.2014.04.031

Paerl H, 2008. Nutrient and other environmental controls of harmful cyanobacterial blooms along the freshwater-marine continuum. In: Hudnell H K (ed). *Cyanobacterial Harmful Algal Blooms: State of the Science and Research Needs*. New York: Springer, 217–237. doi: 10.1007/978-0-387-75865-7_10

Palmer S C J, Odermatt D, Hunter P D et al., 2015. Satellite remote sensing of phytoplankton phenology in Lake Balaton using 10 years of MERIS observations. *Remote Sensing of Environment*, 158: 441–452. doi: 10.1016/j.rse.2014.11.021

Pu J, Song K S, Lv Y F et al., 2022. Distinguishing algal blooms from aquatic vegetation in Chinese lakes using Sentinel 2 image. *Remote Sensing*, 14(9). doi:10.3390/rs14091988

Qin B Q, Xu P Z, Wu Q L et al., 2007. Environmental issues of Lake Taihu, China. *Hydrobiologia*, 581(1): 3–14. doi: 10.1007/s10750-006-0521-5

Ren Y, Pei H Y, Hu W R et al., 2014. Spatiotemporal distribution pattern of cyanobacteria community and its relationship with the environmental factors in Hongze Lake, China. *Environmental Monitoring Assessment*, 186(10): 6919–6933. doi: 10.1007/s10661-014-3899-y

Shi K, Zhang Y L, Zhou Y Q et al., 2017. Long-term MODIS observations of cyanobacterial dynamics in Lake Taihu: responses to nutrient enrichment and meteorological factors. *Scientific Reports*, 7: 40326. doi: 10.1038/srep40326

Simis S G H, Peters S W M, Gons H J, 2005. Remote sensing of the cyanobacterial pigment phycocyanin in turbid inland water. *Limnology and Oceanography*, 50(1): 237–245. doi: 10.4319/lo.2005.50.1.0237

Song K S, Fang C, Jacinthe P A et al., 2021. Climatic versus anthropogenic controls of decadal trends (1983–2017) in algal blooms in lakes and reservoirs across China. *Environmental Science & Technology*, 55(5): 2929–2938. doi: 10.1021/acs.est.0c06480

Stumpf R P, Wynne T T, Baker D B et al., 2012. Interannual variability of cyanobacterial blooms in Lake Erie. *PLoS One*, 7(8): e42444. doi: 10.1371/journal.pone.0042444

Tyler A N, Hunter P D, Carvalho L et al., 2009. Strategies for monitoring and managing mass populations of toxic cyanobacteria in recreational waters: a multi-interdisciplinary approach. *Environmental Health*, 8(S1): S11. doi: 10.1186/1476-069x-8-s1-s11

Wang S L, Li J S, Shen Q et al., 2015. MODIS-based radiometric color extraction and classification of inland water with the forel-ule scale: a case study of Lake Taihu. *IEEE Journal of Selected Topics in Applied Earth Observations and Remote Sensing*, 8(2): 907–918. doi: 10.1109/jstars.2014.2360564

Wang S S, Gao Y N, Li Q et al., 2019. Long-term and inter-monthly dynamics of aquatic vegetation and its relation with environmental factors in Taihu Lake, China. *Science of the Total Environment*, 651: 367–380. doi: 10.1016/j.scitotenv.2018.09.216

Wang Sumin, Dou Hongsheng, 1998. *Annals of Chinese Lakes*. Beijing: Science Press. (in Chinese)

Wells M L, Trainer V L, Smayda T J et al., 2015. Harmful algal blooms and climate change: learning from the past and present to forecast the future. *Harmful Algae*, 49: 68–93. doi: 10.1016/j.hal.2015.07.009

Wells M L, Karlson B, Wulff A et al., 2020. Future HAB science: directions and challenges in a changing climate. *Harmful Algae*, 91: 101632. doi: 10.1016/j.hal.2019.101632

Wynne T T, Stumpf R P, Tomlinson M C et al., 2010. Characterizing a cyanobacterial bloom in western Lake Erie using satellite imagery and meteorological data. *Limnology and Oceanography*, 55(5): 2025–2036. doi: 10.4319/lo.2010.55.5.2025

Xia S, Rua, R Z, Yan M C et al., 2011. Extraction of Hongze Lake reclamation area based on RADARSAT SAR and LANDSAT ETM+. *Procedia Environmental Sciences*, 10: 2294–2300. doi: 10.1016/j.proenv.2011.09.358

Yu W J, Nan Z T, Wang Z W et al., 2015. An effective interpolation method for MODIS land surface temperature on the Qinghai-Tibet Plateau. *IEEE Journal of Selected Topics in Applied Earth Observations and Remote Sensing*, 8(9): 4539–4550. doi: 10.1109/jstars.2015.2464094

Zhang T T, Hu H, Ma X S et al., 2020. Long-term spatiotemporal variation and environmental driving forces analyses of algal blooms in Taihu Lake based on multi-source satellite and land observations. *Water*, 12(4): 1035. doi: 10.3390/w12041035

Zhang Y C, Ma R H, Zhang M et al., 2015. Fourteen-year record (2000–2013) of the spatial and temporal dynamics of floating algae blooms in Lake Chaohu, observed from time series of MODIS images. *Remote Sensing*, 7(8): 10523–10542. doi: 10.3390/rs70810523

Zhao D H, Jiang H, Yang T W et al., 2012. Remote sensing of aquatic vegetation distribution in Taihu Lake using an improved classification tree with modified thresholds. *Journal of Environmental Management*, 95(1): 98–107. doi: 10.1016/j.jenvman.2011.10.007

Zhu Q, Li J S, Zhang F F et al., 2018. Distinguishing cyanobacterial bloom from floating leaf vegetation in Lake Taihu based on medium-resolution imaging spectrometer (MERIS) data. *IEEE Journal of Selected Topics in Applied Earth Observations and Remote Sensing*, 11(1): 34–44. doi: 10.1109/jstars.2017.2757006

Zhu Z, Wulder M A, Roy D P et al., 2019. Benefits of the free and open Landsat data policy. *Remote Sensing of Environment*, 224: 382–385. doi: 10.1016/j.rse.2019.02.016